




**ARTICLE TYPE****This is the sample article title\***Haotian Hong<sup>1</sup>  | Author Two<sup>1</sup>  | Author Three<sup>1,1,1</sup> <sup>1</sup>Org Division, Org Name, State name, Country name<sup>2</sup>Org Division, Org Name, State name, Country name<sup>3</sup>Org Division, Org Name, State name, Country name**Correspondence**

Corresponding author name, This is sample corresponding address. Email: authorone@gmail.com

**Present Address**This is sample for present address text  
this is sample for present address text**Funding Information**

This work was partially supported by National Science Foundation; grant DMS-2014626

**Summary**

This is sample abstract text this is sample abstract text this is sample abstract text this is sample abstract text this is sample abstract text this is sample abstract text

**Purpose:** The aim of this study was to explore the information a 4-pool Bloch-McConnell model provides about the NOE contribution in ischaemic stroke, contrasting that with an intentionally approximate 3-pool model.**Methods:** MRI data from 12 patients presenting with ischaemic stroke were retrospectively analysed, as well as from 6 animals induced with an ischaemic lesion.**Results:** The 4-pool measure of NOEs exhibited a different association with tissue outcome compared to 3-pool approximation in the ischaemic core and in tissue that underwent delayed infarction.**Conclusion:** Associations of NOEs with tissue pathology were found using the 4-pool metric that were not observed using the 3-pool approximation.**KEYWORDS:**

keyword1, keyword2, keyword3, keyword4

**WORD COUNT:** XXX**1 | INTRODUCTION****2 | THEORY**

The extended phase graph (EPG)<sup>?</sup> decompose the magnetization into a series of fourier coefficients in the transverse plane ( $F(k_n)$ ) and longitudinal axis ( $Z(k_n)$ ) in equation ??

$$\begin{cases} F(k_n) &= \frac{1}{2\pi} \int_{-\pi}^{\pi} M_{xy}(\theta) e^{-jn\theta} d\theta, & n \in \mathbb{Z} \\ Z(k_n) &= \frac{1}{2\pi} \int_{-\pi}^{\pi} M_z(\theta) e^{-jn\theta} d\theta, & n \in \mathbb{N} \end{cases} \quad (1)$$

$$k_n = n\phi_{\text{inc}} = n\gamma \int_0^{t_{\text{inc}}} G_{\text{RO}}(\tau) d\tau = n\gamma G_{\text{RO}} t_{\text{inc}} \quad (2)$$

The RF pulse induced rotation of the magnetization could be regarded as independent rotation of each isochromat. The rotation of the  $n$ -th isochromat is given by

\*This is an example for title footnote.

$$\begin{bmatrix} F^+(k_n) \\ F^+(k_{-n}) \\ Z^+(k_n) \end{bmatrix} = \mathbf{R}(\theta, \phi) \begin{bmatrix} F^-(k_n) \\ F^-(k_{-n}) \\ Z^-(k_n) \end{bmatrix} \quad (3)$$

where the rotation matrix  $\mathbf{R}(\theta, \phi)$  is given by

$$\mathbf{R}(\theta, \phi) = \begin{bmatrix} \cos^2 \frac{\alpha}{2} & e^{2i\phi} \sin^2 \frac{\alpha}{2} & -ie^{i\phi} \sin \alpha \\ e^{-2i\phi} \sin^2 \frac{\alpha}{2} & \cos^2 \frac{\alpha}{2} & ie^{-i\phi} \sin \alpha \\ -\frac{i}{2} e^{-i\phi} \sin \alpha & \frac{i}{2} e^{i\phi} \sin \alpha & \cos \alpha \end{bmatrix} \quad (4)$$

The evolution of states between the RF pulses is given by

$$\begin{aligned} F^-(k_{n+1}) &= E_2 F^+(k_n) \\ Z^-(k_{n+1}) &= E_1 Z^+(k_n), \quad n \neq 0 \\ Z^-(k_0) &= E_1 Z^+(k_0) + M_0(1 - E_1) \end{aligned} \quad (5)$$

Under the steady-state condition, the analytic solution for the  $n$ -th coefficient of the transverse magnetization after the RF pulse  $F^+(k_n)$  has been fully investigated by Leupold<sup>?</sup>, which is given by equation ??.

$$F^+(k_n) = \frac{M_0(1 - E_1) \sin \alpha}{(A - BE_2^2)\sqrt{1 - a^2}} \cdot \left[ \left( \frac{\sqrt{1 - a^2} - 1}{a} \right)^{|n|} - E_2 \left( \frac{\sqrt{1 - a^2} - 1}{a} \right)^{|n+1|} \right] \quad (6)$$

where the coefficients  $A$ ,  $B$  and  $a$  are given by

$$\begin{aligned} A &= 1 - E_1 \cos(\alpha) \\ B &= E_1 - \cos(\alpha) \\ a &= \frac{E_2(B - A)}{A - BE_2^2} \end{aligned} \quad (7)$$

The simplified expression for  $F^+(k_{n \geq 0})$  and  $F^+(k_{n < 0})$  is derived as

$$\begin{aligned} F^+(k_{n \geq 0}) &= c(1 - E_2 b) b^n \\ F^+(k_{n < 0}) &= c(1 - E_2 b^{-1}) b^{-n} \end{aligned} \quad (8)$$

where the coefficients  $b$  and  $c$  are given by

$$\begin{aligned} b &= \frac{\sqrt{1 - a^2} - 1}{a} \\ c &= \frac{M_0(1 - E_1) \sin \alpha}{(A - BE_2^2)\sqrt{1 - a^2}} \end{aligned} \quad (9)$$

the echo signal  $S(\text{TE}_n)$  to be measured is given by

$$S_n(\text{TE}_n) = F_n^+ \cdot \underbrace{e^{-\text{TE}_n/T_2}}_{T_2 \text{ relaxation}} \cdot \underbrace{e^{-|\text{TE}_n + n\text{TR}|/T_2'}}_{T_2' \text{ relaxation}} \cdot \underbrace{e^{j\Delta\omega_0(\text{TE}_n + n\text{TR})}}_{\text{off-resonance phase}} \cdot \underbrace{e^{j\{[u(n)-1]\pi - \Delta\psi n\}}}_{\text{RF phase-cycle}} \quad (10)$$

The  $T_2$  and  $T_2'$  relaxation terms scale the transverse magnetization after the RF pulse  $F^+$ . The off-resonance phase term introduce the phase shift of the  $n$ -th echo due to the B0 field inhomogeneity, where  $\Delta\omega_0 = 2\pi\gamma\Delta B_0$ .

The phase-cycle term which was not included in Leupold's paper represent the phase increment of the  $n$ -th echo due to the phase-cycling of the RF pulse, where  $\Delta\psi$  is the phase increment between the RF pulses and  $u(n)$  corresponds to the unit step function.

$$u(n) = \begin{cases} 1, & n \geq 0 \\ 0, & n < 0 \end{cases} \quad (11)$$

The  $B_0$  field map could be estimated by the phase difference between the echoes.

In our sequence, we acquire adjacent echoes with fixed echo spacing  $\Delta\text{TE}$ . The signal intensity of the  $n$ -th echo is expressed as  $\text{TE}_n = \text{TE}_0 + n\Delta\text{TE}$

The logarithm of the signal intensity is linearly related to  $n$ . For simplicity, we replace the linear coefficient term with  $\mu^+$  and  $\mu^-$ , and the residual term with  $\lambda^+$  and  $\lambda^-$ .

$$\log [|S(\text{TE}_n)|] = \log (|F^+(k_n)|) - \frac{\text{TE}_n}{T_2} - \frac{|\text{TE}_n + n\text{TR}|}{T_2'} \quad (12)$$

$$\begin{aligned} \log [|S(\text{TE}_{n \geq 0})|] &= \log [c(1 - E_2 b)] + n \log(b) - \frac{\text{TE}_n}{T_2} - \frac{\text{TE}_n + n\text{TR}}{T_2'} \\ &= \left[ \log(b) - \frac{\Delta\text{TE}}{T_2} - \frac{\Delta\text{TE} + \text{TR}}{T_2'} \right] n + \left\{ \log [c(1 - E_2 b)] - \frac{\text{TE}_0}{T_2} - \frac{\text{TE}_0 + \text{TR}}{T_2'} \right\} \\ &= \lambda^+ n + \mu^+ \end{aligned} \quad (13)$$

$$\begin{aligned} \log [|S(\text{TE}_{n < 0})|] &= \log [-c(1 - E_2 b^{-1})] - n \log(b) - \frac{\text{TE}_n}{T_2} + \frac{\text{TE}_n + n\text{TR}}{T_2'} \\ &= \left[ -\log(b) - \frac{\Delta\text{TE}}{T_2} + \frac{\Delta\text{TE} + \text{TR}}{T_2'} \right] n + \left\{ \log [-c(1 - E_2 b^{-1})] - \frac{\text{TE}_0}{T_2} + \frac{\text{TE}_0 + \text{TR}}{T_2'} \right\} \\ &= \lambda^- n + \mu^- \end{aligned} \quad (14)$$

The total signal intensity of the echoes is given by

$$\begin{aligned} \sum_{n=-\infty}^{\infty} |S(\text{TE}_n)| &= \sum_{n=0}^{\infty} e^{\lambda^+ n + \mu^+} + \sum_{n=-\infty}^{-1} e^{\lambda^- n + \mu^-} \\ &= \frac{e^{\mu^+}}{1 - e^{\lambda^+}} + \frac{e^{\mu^-}}{e^{\lambda^-} - 1} \\ &= \frac{c(1 - E_2 b) e^{-\text{TE}_0/T_2 - \text{TE}_0/T_2'}}{1 - b e^{-\Delta\text{TE}/T_2 + (\Delta\text{TE} + \text{TR})/T_2'}} + \frac{-c(1 - E_2 b^{-1}) e^{-\text{TE}_0/T_2 + \text{TE}_0/T_2'}}{b^{-1} e^{-\Delta\text{TE}/T_2 + (\Delta\text{TE} + \text{TR})/T_2'}} \end{aligned}$$

The magnitude sum of all the echoes is different from the signal intensity of the bSSFP sequence. The bSSFP image contrast as well as the banding artifacts could be readily generated by the complex sum of the echoes. The dark band is due to the phase cancellation from

$$S_{\text{bSSFP(banding)}} = \sum_{n=-\infty}^{\infty} S(\text{TE}_n)$$

$$= \sum_{n=0}^{\infty} e^{\lambda^+ n + \mu^+ + j[\Delta\omega_0(\text{TE}_n + n\text{TR}) - \Delta\psi n]} + \sum_{n=-\infty}^{-1} e^{\lambda^- n + \mu^- + j[\Delta\omega_0(\text{TE}_n + n\text{TR}) + \pi - \Delta\psi n]}$$

$$= \frac{e^{\mu^+ + j\Delta\omega_0 \text{TE}_0}}{1 - e^{\lambda^+ + j[\Delta\omega_0(\Delta\text{TE} + \text{TR}) - \Delta\psi]}} + \frac{e^{\mu^- + j\Delta\omega_0 \text{TE}_0}}{1 - e^{\lambda^- + j[\Delta\omega_0(\Delta\text{TE} + \text{TR}) + \Delta\psi]}}$$

To generate the bSSFP image contrast without banding from the MESS echoes, it's straightforward to neglect the off-resonance phase term. The phase-cycle term should be preserved to maintain the image contrast.

$$S_{\text{bSSFP(no banding)}} = \sum_{n=-\infty}^{\infty} |S(\text{TE}_n)| e^{\{[u(n)-1]\pi - \Delta\psi n\}} = \sum_{n=0}^{\infty} e^{\lambda^+ n + \mu^+ + j[\Delta\omega_0(\text{TE}_n + n\text{TR}) - \Delta\psi n]} + \sum_{n=-\infty}^{-1} e^{\lambda^- n + \mu^- + j[\Delta\omega_0(\text{TE}_n + n\text{TR}) + \pi - \Delta\psi n]}$$

$$= \frac{e^{\mu^+}}{1 - e^{\lambda^+ - j\Delta\psi}} + \frac{e^{\mu^-}}{1 - e^{\lambda^- - j\Delta\psi}}$$

## 3 | METHODS

### 3.1 | Pulse Sequence Generation

### 3.2 | Simulation Experiments

### 3.3 | Phantom and In Vivo Experiments

## 4 | RESULTS

## 5 | DISCUSSION

## 6 | CONCLUSION

## ACKNOWLEDGMENTS

### Author contributions

This is an author contribution text. This is an author contribution text. This is an author contribution text. This is an author contribution text. This is an author contribution text.

### Financial disclosure

None reported.

### Conflict of interest

The authors declare no potential conflict of interests.

## SUPPORTING INFORMATION

The following supporting information is available as part of the online article:

**Figure S1.** 500 hPa geopotential anomalies for GC2C calculated against the ERA Interim reanalysis. The period is 1989–2008.

**Figure S2.** The SST anomalies for GC2C calculated against the observations (OIsst).

**How to cite this article:** Williams K., B. Hoskins, R. Lee, G. Masato and T. Woollings (2016), A regime analysis of Atlantic winter jet variability applied to evaluate HadGEM3-GC2, *Magn. Reson. Med.*, 2017;00:1–6.

## APPENDIX

### A SECTION TITLE OF FIRST APPENDIX

Use `\begin{verbatim}...\end{verbatim}` for program codes without math. Use `\begin{alltt}...\end{alltt}` for program codes with math. Based on the text provided inside the optional argument of `\begin{code}[Pseudocode|Listing|Box|Code|Specification|Procedure|Sourcecode|Program]...\end{code}` tag corresponding boxed like floats are generated. Also note that `\begin{code}[Code|Listing]...\end{code}` tag with either Code or Listing text as optional argument text are set with computer modern typewriter font. All other code environments are set with normal text font. Refer below example:

**Listing 1** Descriptive Caption Text

```
for i:=maxint to 0 do
begin
{ do nothing }
end;
Write('Case insensitive ');
WritE('Pascal keywords.');
```

### A.1 Subsection title of first appendix

Nam dui ligula, fringilla a, euismod sodales, sollicitudin vel, wisi. Morbi auctor lorem non justo. Nam lacus libero, pretium at, lobortis vitae, ultricies et, tellus. Donec aliquet, tortor sed accumsan bibendum, erat ligula aliquet magna, vitae ornare odio metus a mi.

## A.1.1 Subsection title of first appendix

### Unnumbered figure

Fusce mauris. Vestibulum luctus nibh at lectus. Sed bibendum, nulla a faucibus semper, leo velit ultricies tellus, ac venenatis arcu wisi vel nisl. Vestibulum diam. Aliquam pellentesque, augue quis sagittis posuere, turpis lacus congue quam, in hendrerit risus eros eget felis. Maecenas eget erat in sapien mattis porttitor. Vestibulum porttitor. Nulla facilisi. Sed a turpis eu lacus commodo facilisis. Morbi fringilla, wisi in dignissim interdum, justo lectus sagittis dui, et vehicula libero dui cursus dui. Mauris tempor ligula sed lacus. Duis cursus enim ut augue. Cras ac magna. Cras nulla.

## B SECTION TITLE OF SECOND APPENDIX

Fusce mauris. Vestibulum luctus nibh at lectus. Sed bibendum, nulla a faucibus semper, leo velit ultricies tellus, ac venenatis arcu wisi vel nisl.

### B.1 Subsection title of second appendix

Sed commodo posuere pede. Mauris ut est. Ut quis purus. Sed ac odio. Sed vehicula hendrerit sem. Duis non odio. Morbi ut dui. Sed accumsan risus eget odio. In hac habitasse platea dictumst. Pellentesque non elit. Fusce sed justo eu urna porta tincidunt. Mauris felis odio, sollicitudin sed, volutpat a, ornare ac, erat. Morbi quis dolor. Donec pellentesque, erat ac sagittis semper, nunc dui lobortis purus, quis congue purus metus ultricies tellus. Proin et quam. Class aptent taciti sociosqu ad litora torquent per conubia nostra, per inceptos hymenaeos. Praesent sapien turpis, fermentum vel lacus.

#### B.1.1 Subsection title of second appendix

Lorem ipsum dolor sit amet, consectetur adipiscing elit. Ut purus elit, vestibulum ut, placerat ac, adipiscing vitae, felis. Curabitur dictum gravida mauris. Nam arcu libero, nonummy eget, consectetur id, vulputate a, magna. Donec vehicula augue eu neque. Pellentesque habitant morbi tristique senectus et netus et malesuada fames ac turpis egestas.

$$\mathcal{L} = i\bar{\psi}\gamma^\mu D_\mu\psi - \frac{1}{4}F_{\mu\nu}^a F^{a\mu\nu} - m\bar{\psi}\psi \quad (\text{B1})$$

Quisque ullamcorper placerat ipsum. Cras nibh. Morbi vel justo vitae lacus tincidunt ultrices. Lorem ipsum dolor sit amet, consectetur adipiscing elit. In hac habitasse platea dictumst. Integer tempus convallis

augue. Etiam facilisis. Nunc elementum fermentum wisi. Lorem ipsum dolor sit amet, consectetur adipiscing elit. In hac habitasse platea dictumst. Integer tempus convallis augue. Etiam facilisis. Nunc elementum fermentum wisi. Quisque ullamcorper placerat ipsum. Cras nibh. Morbi vel justo vitae lacus tincidunt ultrices. Lorem ipsum dolor sit amet, consectetur adipiscing elit. In hac habitasse platea dictumst. Integer tempus convallis augue. Etiam facilisis. Nunc elementum fermentum wisi. Aenean placerat. Ut imperdiet, enim sed gravida sollicitudin, felis odio placerat quam, ac pulvinar elit purus eget enim. Nunc vitae tortor. Proin tempus nibh sit amet nisl. Vivamus quis tortor vitae risus porta vehicula.

col1 head	col2 head	col3 head
col1 text	col2 text	col3 text
col1 text	col2 text	col3 text
col1 text	col2 text	col3 text

Quisque ullamcorper placerat ipsum. Cras nibh. Morbi vel justo vitae lacus tincidunt ultrices. Lorem ipsum dolor sit amet, consectetur adipiscing elit. In hac habitasse platea dictumst. Integer tempus convallis augue. Etiam facilisis. Nunc elementum fermentum wisi. Aenean placerat. Ut imperdiet, enim sed gravida sollicitudin, felis odio placerat quam, ac pulvinar elit purus eget enim. Nunc vitae tortor. Proin tempus nibh sit amet nisl. Vivamus quis tortor vitae risus porta vehicula.

Fusce mauris. Vestibulum luctus nibh at lectus. Sed bibendum, nulla a faucibus semper, leo velit ultricies tellus, ac venenatis arcu wisi vel nisl. Vestibulum diam. Aliquam pellentesque, augue quis sagittis posuere, turpis lacus congue quam, in hendrerit risus eros eget felis. Maecenas eget erat in sapien mattis porttitor. Vestibulum porttitor. Nulla facilisi. Sed a turpis eu lacus commodo facilisis. Morbi fringilla, wisi in dignissim interdum, justo lectus sagittis dui, vehicula libero dui cursus dui. Mauris tempor ligula sed lacus. Duis cursus enim ut augue. Cras ac magna. Cras nulla. Nulla egestas. Curabitur a leo. Quisque egestas wisi eget nunc. Nam feugiat lacus vel est. Curabitur consectetur.

Pellentesque habitant morbi tristique senectus et netus et malesuada fames ac turpis egestas. Donec odio elit, dictum in, hendrerit sit amet, egestas sed, leo. Praesent feugiat sapien aliquet odio. Integer vitae

**TABLE B1** This is an example of Appendix table showing food requirements of army, navy and airforce.

col1 head	col2 head	col3 head
col1 text	col2 text	col3 text
col1 text	col2 text	col3 text
col1 text	col2 text	col3 text

01	justo. Aliquam vestibulum fringilla lorem. Sed neque	54
02	lectus, consectetur at, consectetur sed, eleifend ac,	55
03	lectus. Nulla facilisi. Pellentesque eget lectus. Proin eu	56
04	metus. Sed porttitor. In hac habitasse platea dictumst.	57
05	Suspendisse eu lectus.	58
06		59
07		60
08		61
09		62
10		63
11		64
12		65
13		66
14		67
15		68
16		69
17		70
18		71
19		72
20		73
21		74
22		75
23		76
24		77
25		78
26		79
27		80
28		81
29		82
30		83
31		84
32		85
33		86
34		87
35		88
36		89
37		90
38		91
39		92
40		93
41		94
42		95
43		96
44		97
45		98
46		99
47		100
48		101
49		102
50		103
51		104
52		105
53		106